Catalytic Deracemization of *α*-Branched Aldehydes *via* Visible Light Promoted *E*/*Z* Isomerization of Enamine Intermediate

Mouxin Huang, Long Zhang, Tianrun Pan, Sanzhong Luo*

Center of Basic Molecular Science, Department of Chemistry, Tsinghua University, Beijing, 100084, China

*Corresponding author. Email: luosz@tsinghua.edu.cn.

Abstract: Catalytic deracemization of *α*-branched aldehydes represents an unmet challenge with fundamental importance in carbonyl chemistry. In this work, we report a photochemical *E*/*Z* isomerization strategy for the deracemization of *α*-branched aldehydes by using simple aminocatalysts and readily available photosensitizers. Various racemic *α*-branched aldehydes could be directly transformed into their corresponding single enantiomers in high enantioselectivity. Rapid photodynamic *E*/*Z* isomerization and highly stereospecific iminium/enamine tautomerization are two key factors that facilitate the highly effective enantio-enrichment. This study presents a distinctive photochemical *E*/*Z* isomerizing strategy for externally tuning enamine catalysis.

One-Sentence Summary: Catalytic deracemization is arguably the most straightforward strategy in constructing chiral *α*-tertiary carbonyls, which are essential to pharmaceutic and biological applications. Despite the tremendous advances in stereogenic carbonyl reactions, catalytic deracemization of *α*-tertiary carbonyls has not been achieved due to their tendency of racemization as well as the inherent thermodynamic and kinetic constraints for such a process. We report herein a distinctive photochemical *E*/*Z* isomerization strategy for catalytic deracemization of *α*-branched aldehydes. The joint force of chiral primary amine and photosensitizer facilitated highly effective enantio-enrichment for a range of racemic *α*-branched aldehydes.

Main Text:

Carbonyl transformations are text-book reactions and their catalytic asymmetric versions are continuingly developed to provide enantiomerically pure products that are essential to pharmaceutic and biological applications (*1*, *2*). Most of these methods involve stereogenic C-C/C-X bond formations featuring enol- or enamine-based processes, wherein the geometry of the intermediate and its facial selectivity during bond formation dictate the stereoselectivity (*3*, *4*) (Fig. 1A). In the construction of chiral *α*-tertiary carbonyls, catalytic deracemization is arguably the most straightforward strategy because it directly transfers a racemic compound into its enantiomerically pure form (*5*). However, to develop deracemization of *α*-tertiary carbonyls remains an elusive aim despite tremendous progress in stereogenic carbonyl transformations (*6*, *7*). The challenges are triple folds. First, deracemization is inherently endergonic with a negative entropy change. In addition, according to the principle of microscopic reversibility (*8*), the backward and forward pathway is identical for a given chiral catalytic cycle. Hence, the enantio-enriched status of the starting material could not be adjusted *via* an existing catalytic pathway without any exogenous chemical or physical inputs (Fig. 1A). Recent seminal works by Bach (*9*, *10*), Knowles & Miller (*11*) have demonstrated that light irradiation could supply the necessary external perturbation that broke the thermodynamic and kinetic constraints. Accordingly, photo-mediate energy transfer and electron-transfer were found to work effectively in the context of chiral catalysts to facilitate enantioselective deracemization of allene or cyclic urea, respectively (Fig. 1B). Last but not the least, *α*-tertiary carbonyls such as *α*-tertiary aldehydes are easily racemized *via* non-controlled by-pathways, adding more complexity in pursuing catalytic deracemization (*12*, *13*).

Bearing these challenges in mind, we herein reported a photochemical *E*/*Z* isomerization strategy for the deracemization of *α*-branched aldehydes by using simple aminocatalysts and readily available photosensitizers (Fig. 1C). Photo-isomerization was found to perturb the *E*/*Z* population of the *in-situ* generated enamine intermediate. This photochemical strategy together with our previous finding (*14*, *15*) that enamine formation with chiral primary amine catalyst such as **1a** is highly stereospecific, makes possible a highly enantioselective deracemization process. It should be noted that though visible light promoted *E*/*Z* isomerization of double bond was widely applied in chemical (*16*) and material science (*17*), such a process with a transient catalytic intermediate has not been achieved in pursuing stereoselective catalysis. Photochemical tuning of enamine intermediate has been explored in the pioneering studies by MacMillan (*18*, *19*) and Melchiorre (*20*, *21*) using photo-induced electron-transfer, which significantly expanded the capacity of nucleophilic enamine catalysis. Our current strategy complements these known processes by harnessing the *E*/*Z* photo-isomerziation property of enamine double bond.

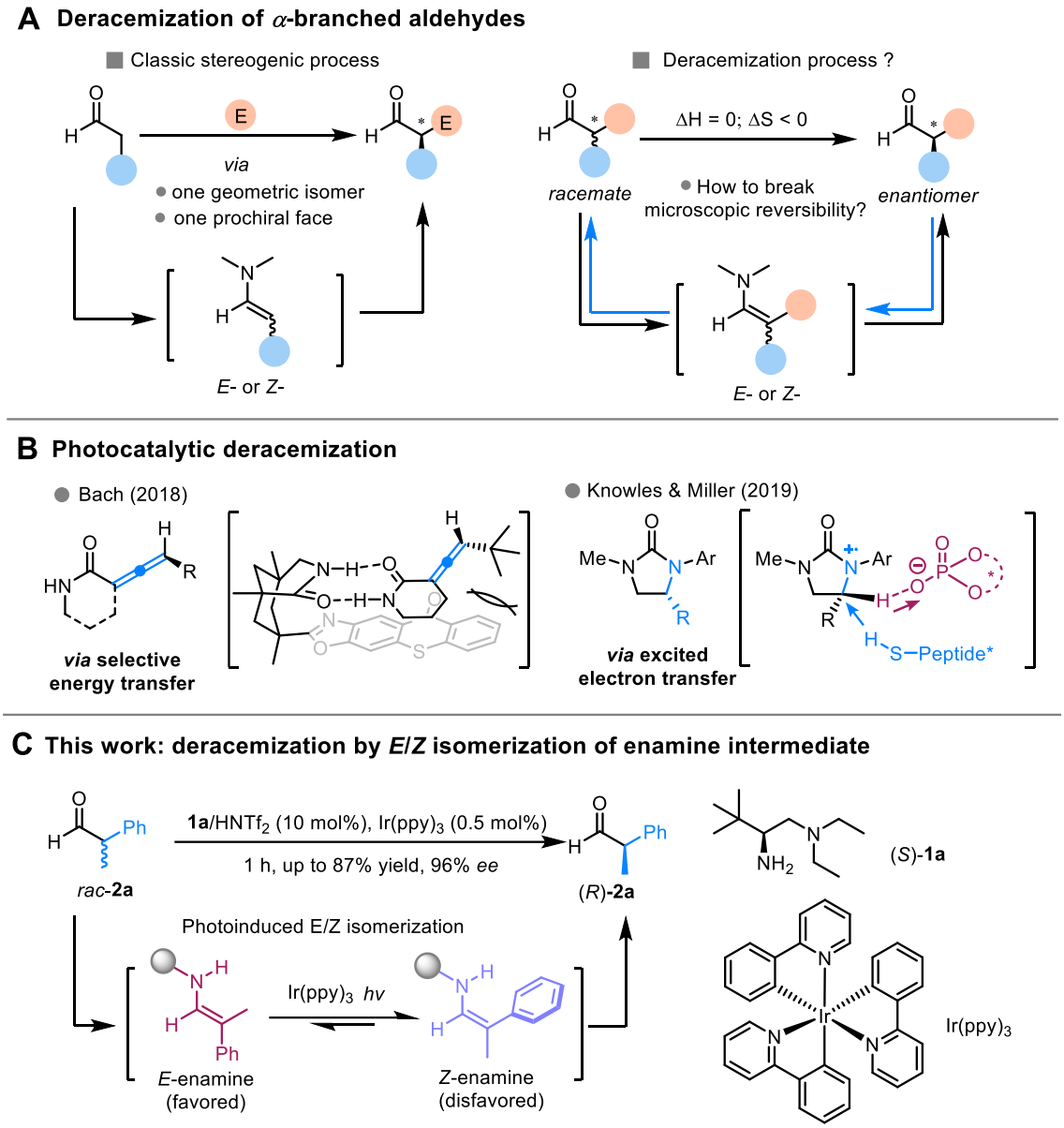

Figure 1. Deracemization *via* energy transfer catalysis. (A) Asymmetric carbonyl transformation. **(B)** Prior works on photocatalytic deracemization. **(C)** Deracemization of α-branched aldehydes *via* photochemical *E*/*Z* isomerization of enamine intermediate.

We first investigated the deracemization of 2-phenylpropionaldehyde **2a** based on the chiral primary-amine catalysis (*14*). Photocatalysts showed dramatic impact on optical enrichment (Table. S2) and $Ir(ppy)_3$ was identified as the optimal photocatalyst. The addition of weak acid such as benzoic acid could significantly improve the enantioselectivity (Fig. 2, entry 2), consistent with our previous finding on stereoselective enamine protonation (*15*). With $Ir(ppy)_3$, benzoic acid and primary-tertiary amine (*S*)-**1a**/$HNTf_2$, the deracemization completed rapidly in 1 h to afford (*R*)-**2a** in 77% yield (73% isolated yield) and 94% *ee*. Control experiments indicated that aminocatalyst, photocatalyst and light irradiation were all essential and their absence led to no enrichment or rather poor enantioselectivity (entry 1 *vs* 3 and 4). The minor yet noticeable enantioselectivity observed under thermo-conditions (entries 3 and 4) could be

accounted by considering kinetic resolution *via* selective trapping of aldehyde by aminocatalyst (Fig. S2 and S3, ca. 10%). This also explains the loss of aldehyde during this process. We next examined the reactions with optically pure aldehydes. Both (*R*)- and (*S*)-**2a** led to (*R*)-selectivity with comparable enantioselectivity (Fig. 2C, entries 7 and 8). In contrast, racemization was observed without light irradiation in these cases. This observation strongly suggests that light supplies the major driving force for the current deracemization reaction. It was found that the addition of *E*-stilbene or conducting the reaction in the presence of oxygen, well-known energy transfer quenchers, completely inhibited the deracemization (Fig. 2B, entries 5 and 6), a strong indication of the energy transfer mechanism.

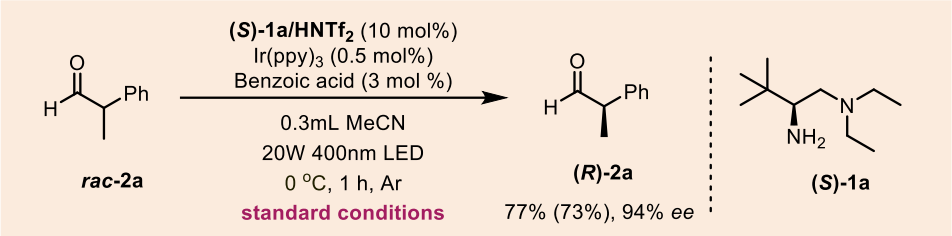

A **Control experiment**

Entry	Variation	Yield (%)	ee (%)
1	No **1a**	99	rac
2	No benzoic acid	76	42
3	No $Ir(ppy)_3$	65	19

B **Triplet state inhibitor**

Entry	Variation	Yield (%)	ee (%)
4	No light	58	13
5	Under air	51	39
6	1 equiv *E*-stilbene	64*	20

C **With optically pure substrates**

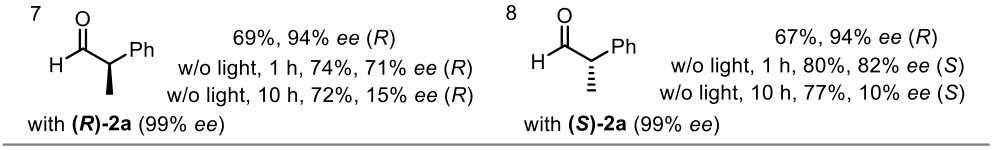

Figure 2. Reaction development. (A) Control experiments. Reactions were performed on a 0.2 mmol scale. The yields were determined by GC analysis with biphenyl as an internal standard. The data in parentheses refers to isolated yield. The *ee* values were determined by HPLC analysis. **(B)** The effect of triplet state inhibitor. *The resulting *E*/*Z* ratio of stilbene was 1:2.5. **(C)** Deracemization performed with optical pure substrates.

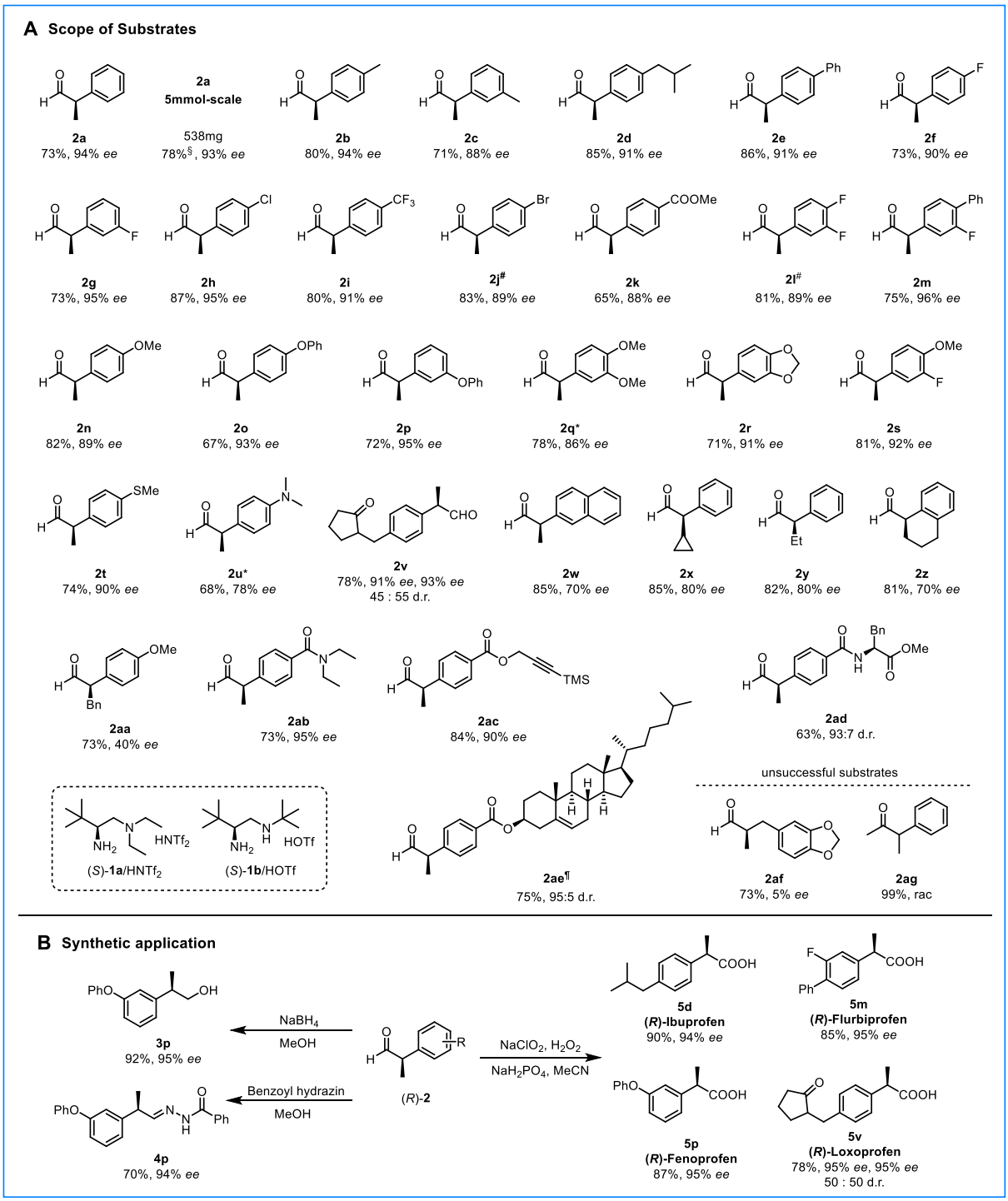

Figure 3. Substrate scope and synthetic application. (A) Substrate scope. Reactions were performed on a 0.2 mmol scale. The yields are of isolated material after purification. §The yield was determined from the corresponding alcohol. *(*S*)-**1b**/HOTf instead of (*S*)-**1a**/$HNTf_2$. # $Ir(F\text{-}ppy)_3$ instead of $Ir(ppy)_3$. ¶DCM instead of MeCN as the solvent. **(B)** Synthetic application. Reactions were performed on a 0.1 mmol scale.

The scope of this deracemization was next examined (Fig. 3A). 2-Arylpropanals bearing alkyl or aryl groups at the aromatic ring such as Me, *i*-Bu and Ph (**2a**-**e**) gave high enantioselectivities. Both electron-deficient substituents such as halogen, trifluoromethyl and

carboxylate (**2f-m**) and electron-donating groups such as alkoxyl, aryloxy and methylenedioxy groups (**2n-s**) gave consistently high enantioselectivity. Functional groups such as methylthio (**2t**) and dimethylamino moiety (**2u**) also worked well. When aldehyde and ketone coexisted in the same compound, deracemization would occur preferentially on α-carbon of aldehyde while ketone moiety remained intact (**2v**). Expanding the aromatic ring or increasing size of the branched chain led to a slight reduction of enantioselectivity (**2w-aa**). The current deracemization could also be applied to complex arylaldehydes bearing functional groups such as amide and alkynes (**2ab**, **2ac**) and existing chiral centers such as amino acid and steroid (**2ad**, **2ae**). Aliphatic aldehydes other than 2-arylacetaldehyde skeleton showed low enantio-enrichment (**2af**), the preference to the latter can be rationalized by considering the requirement of aryl alkene chromophore in the forming enamine for photoisomerization (*22*). An α-branched ketone was also examined, showing unfortunately no enantio-enrichment (**2ag**). Delightfully, a 5 mmol-scale reaction of **2a** performed equally well, delivering a similar outcome. To demonstrate the synthetic utility of the reaction, we executed simple oxidation of selected examples to obtain nonsteroidal anti-inflammatory drugs without loss of enantioselectivity. The aldehydes could also perform reduction and condensation with maintaining enantioselectivity (Fig. 3B).

A Comparision of various photocatalysts

Photocatalyst	E_T (kcal/mol)	$E_{1/2}^{PC+/PC*}$(V)	ee (%)
Thioxanthone	64.4	+1.18	64
Ir(dFCF$_3$ppy)$_2$dtbppyPF$_6$	61.8	+1.21	73
Ir(ppy)$_3$	58.1	+0.31	94
Ir(pCF$_3$-ppy)$_3$	56.4	+0.59	93
2,4,6-triphenylpyrylium	53.0	+2.02	18
Ru(bpy)$_3$Cl$_2$·6H$_2$O	46.5	+0.77	39
E-enamine	54.4	+0.73*	

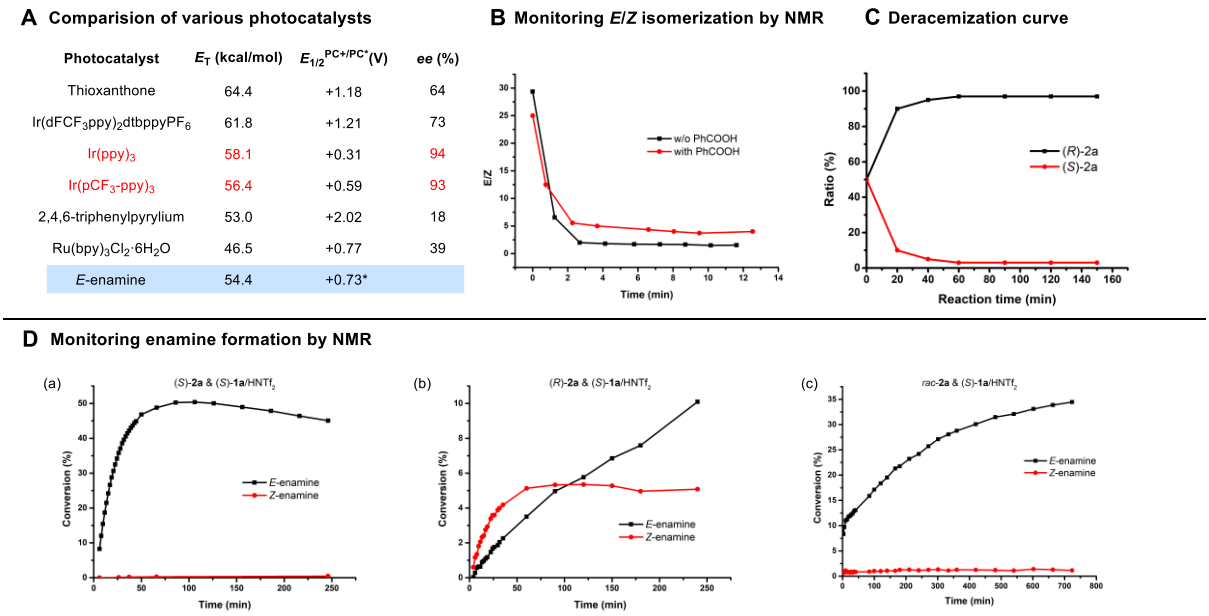

Figure 4. Mechanistic experiments. (A) Investigation of the performance of various photosensitizers. *E_{ox} value instead of $E_{1/2}^{PC+/PC*}$. **(B)** Monitoring the ratio of *E*/*Z*-enamine by *in-situ* irradiation in NMR detector. The starting material was pre-equilibrated to attain an equilibrium ratio of *E*/*Z*-enamine. Conditions: (*S*)-**1a**/HNTf$_2$ (0.067 M), **2a** (0.067 M), benzoic acid (20 mol %) and Ir(ppy)$_3$ (2.5 mol %) in 0.6 mL MeCN-d_3, pre-equilibrated for 10 h, then 405 nm laser irradiation inside NMR detector for 20 min. Details are included in the supplementary materials (Fig. S9-11). **(C)** Time-course profile for deracemization under the standard conditions. (**D**) Monitoring the enamine formation process by NMR: (a) with (*S*)-**2a**;

(b) with (*R)*-**2a**; (c) with *rac*-**2a**. Conditions: (*S*)-**1a**/$HNTf_2$ (0.067 M) and **2a** (0.067 M) in 0.6 mL MeCN-d_3 with PhCOOBn as the internal standard.

In our deracemization process, the photochemical perturbation may proceed *via* electron-transfer (followed by hydrogen-transfer) or energy transfer induced isomerization. The redox potential of *E*- or *Z*-enamine intermediate was determined to be 0.73 V (*23*), while $Ir(ppy)_3$ has $E_{1/2}^{PC+/PC*}$ = 0.31 V. Though PET between enamine and photocatalyst is possible, this was discounted as the obtained enantioselectivity seems not related to the excited-state redox potential, but triple-state energy (E_T) as revealed in the screening of different photocatalysts (Fig. 4A). High enantioselectivity was generally obtained with triplet-state energy of photocatalysts in the range of 56-59 kcal/mol, which is in line with the triplet-state energy of enamine intermediate, 54.4 kcal/mol (Fig. 5B). The observed inhibition effect with typical triplet-state inhibitors such as stilbene or oxygen provides further supports to an energy-transfer mechanism.

Stoichiometric experiments were conducted to examine the enamine formation by NMR (Fig. 4D, S5-8). The joint use of a strong acid $HNTf_2$ and a weak benzoic acid could significantly enhance the rate of iminium-enamine tautomerization as known (Fig. S5) (*14*). In the presence of (*S*)-**1a**/$HNTf_2$, it was found that (*S*)-**2a** selectively formed *E*-enamine equilibrating at about 50% conversion (Fig. 4D, a), while (*R*)-**2a** preferentially gave *Z*-enamine which was equilibrated at rather lower conversion (ca. 5%) (Fig. 4D, b), and an overriding formation of *E*-enamine was observed further on. We also examined enamine formation with *rac*-**2a**, showing similar kinetic profile with that of (*S*)-**2a**, with *E*-enamine as the major isomer (*E*/*Z* = 30:1, equilibrated at ca. 35% conversion) (Fig. 4D, c). These results suggested that (*S*)-**2a** and (*S*)-**1a** are stereochemically matched with each other and their coupling led to the formation of *E*-enamine, which is favored both thermodynamically and kinetically.

Moreover, enamine isomerization was investigated by an *in-situ* irradiative NMR experiment. A 405nm laser beam was imported into a pre-equilibrated reaction mixture by optical fiber inside the NMR detector. *E*-enamine was found to isomerize into *Z*-enamine rapidly, and a photo-stationary state was reached within three minutes with *E*/*Z*-enamine ratio maintaining at 1.7:1 or 4:1, depending on the existence of acid additive (Fig. 4B). Quenching study verified that the excited photocatalyst could be selectively quenched by enamine (Fig. S13-15). We also tracked the reaction progress of deracemization and a photodynamic equilibration could be established in one hour with 94% *ee* (Fig. 4C). The enantioselectivity did not change upon extending irradiation, but turning off light led to immediate racemization (Fig. S16). This observation proved that the deracemization was driven by photocatalytic enamine isomerization.

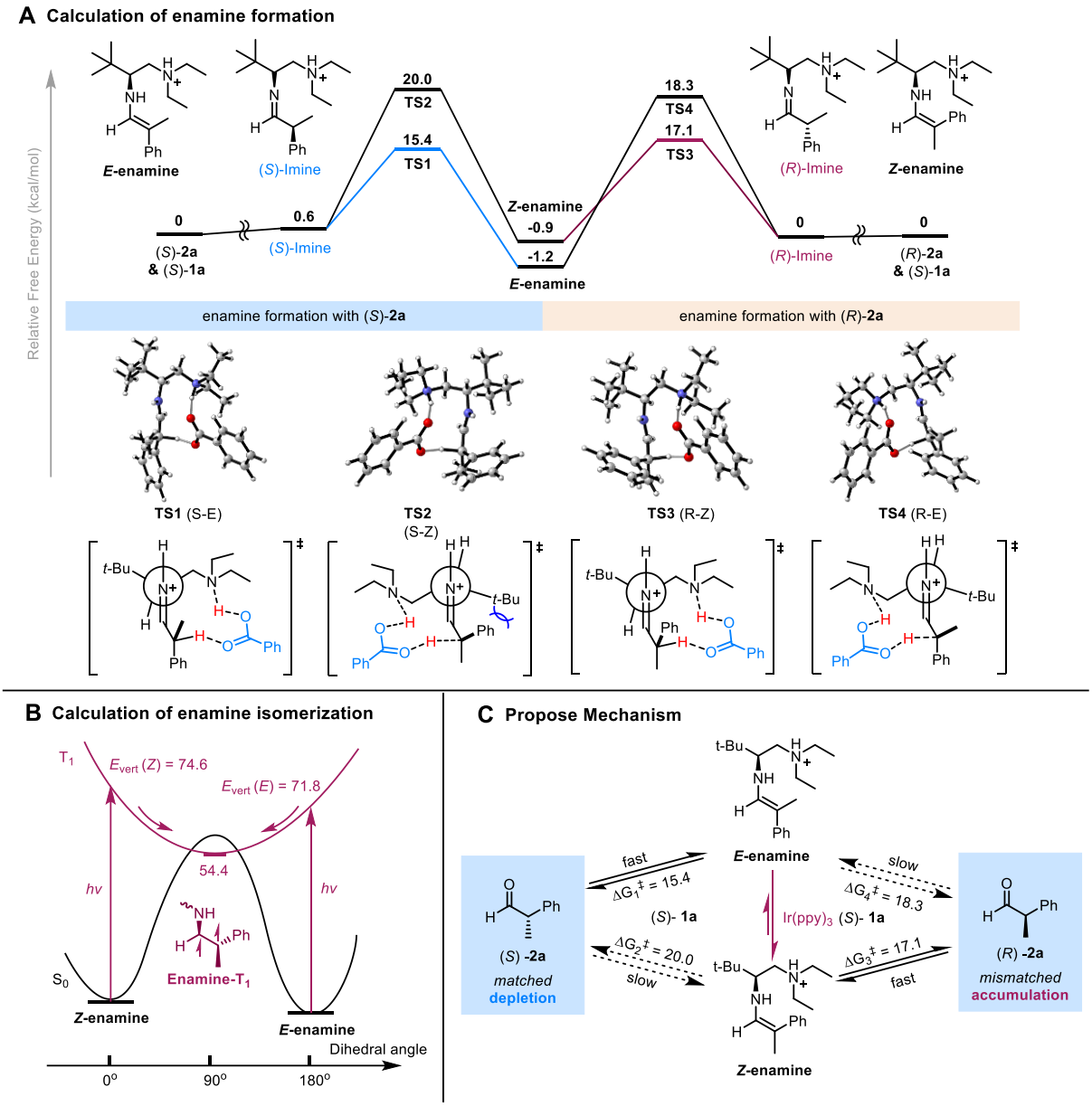

Figure 5. DFT Calculation studies and proposed mechanism. (A) Calculation of enamine formation process. **(B)** Calculation of enamine isomerization process. **(C)** Proposed mechanism.

We further rationalized the mechanism by DFT calculations. Based on previous work, a weak-acid-bridged proton transfer pathway was proposed to account for the iminium-enamine tautomerization (*24*). We calculated all four possible transition states (**TS 1-4**) leading to *E*- and *Z*- enamine (Fig. 5A). It was found that (*S*)-**2a** formed *E*-enamine selectively (**TS1** *vs* **TS2**) with $\Delta\Delta G_{21}$ = 4.6 kcal/mol, while (*R*)-**2a** showed moderate preference for *Z*-enamine **(TS3** *vs* **TS4**) with $\Delta\Delta G_{43}$ = 1.2 kcal/mol. These results are in full consistence with the experimentally observed kinetic profile of enamine formation (Fig. 4D). According to the principle of microscopic reversibility (*8*), the backward enamine protonation may proceed *via* **TS1** and **TS4** for *E*-enamine and *via* **TS2** and **TS3** for *Z*-enamine, both processes were of the same selectivity

with $\Delta\Delta G_{41}$ and $\Delta\Delta G_{32}$ were both equal to 2.9 kcal/mol. Hence, the protonation of *E*- or *Z*-enamine was highly facial selective in producing (*S*)-**2a** or (*R*)-**2a**, respectively. The vertical excitation energies ($S_0 \rightarrow T_1$) for *E*/*Z* enamine were calculated to be 71.8 and 74.6 kcal/mol favoring excitation of *E*-enamine (Fig. 5B). The preferential excitation of *E*-enamine over *Z*-enamine could be explained by the decojugation of *β*-enaminyl phenyl group in the *Z*-geometry due to space hindrance. Recently, similar deconjugation effect has also been observed in visible-light promoted isomerization of *E*-alkenes to their thermodynamically disfavored *Z*-isomers (*25*-*27*).

On the basis of the mechanistic investigations above, a plausible mechanism for optical enrichment was proposed (Fig. 5C). Under the ground-state, the stereochemically matched enantiomer forms a dominant *E*-configured enamine, which is continuingly isomerized to its disfavored *Z*-isomer *via* photocatalytic energy transfer. Facial selective protonation of *Z*-enamine then delivers mismatched enantiomer. Hence, the consumption of the matched enantiomer and accumulation of the mismatched enantiomer are sustained to facilitate effective deracemization. In this process, the stereo-specificity of enamine protonation by chiral primary aminocatalysis is also a critical determinant for effective optical enrichment.

References and Notes

1. S. E. Denmark, J. R. Heemstra Jr, G. L. Beutner, Catalytic, Enantioselective, Vinylogous Aldol Reactions. *Angew. Chem. Int. Ed.* **44**, 4682-4698 (2005).
2. B. Schetter, R. Mahrwald, Modern Aldol Methods for the Total Synthesis of Polyketides. *Angew. Chem. Int. Ed.* **45**, 7506-7525 (2006).
3. S. Mukherjee, J. W. Yang, S. Hoffmann, B. List, Asymmetric enamine catalysis. *Chem. Rev.* **107**, 5471-5569 (2007).
4. Y. Yamashita, T. Yasukawa, W.-J. Yoo, T. Kitanosono, S. Kobayashi, Catalytic enantioselective aldol reactions. *Chem. Soc. Rev.* **47**, 4388-4480 (2018).
5. K. Faber, Non-Sequential Processes for the Transformation of a Racemate into a Single Stereoisomeric Product: Proposal for Stereochemical Classification. *Chem. Eur. J.* **7**, 5004-5010 (2001).
6. M. Rueping, A. Kuenkel, I. Atodiresei, Chiral Brønsted acids in enantioselective carbonyl activations – activation modes and applications. *Chem. Soc. Rev*. **40**, 4539-4549 (2011).
7. S. Afewerki, A. Córdova, Combinations of Aminocatalysts and Metal Catalysts: A Powerful Cooperative Approach in Selective Organic Synthesis. *Chem. Rev*. **116**, 13512-13570 (2016).
8. D. G. Blackmond, "If pigs could fly" chemistry: a tutorial on the principle of microscopic reversibility. *Angew. Chem. Int. Ed.* **48**, 2648-2654 (2009).
9. A. Holzl-Hobmeier *et al*., Catalytic deracemization of chiral allenes by sensitized excitation with visible light. *Nature* **564**, 240-243 (2018).
10. M. Plaza, C. Jandl, T. Bach, Photochemical Deracemization of Allenes and Subsequent Chirality Transfer. *Angew. Chem. Int. Ed.* **59**, 12785-12788 (2020).

11. N. Y. Shin, J. M. Ryss, X. Zhang, S. J. Miller, R. R. Knowles, Light-driven deracemization enabled by excited-state electron transfer. *Science* **366**, 364-369 (2019).
12. F. Agbossou, J.-F. Carpentier, A. Mortreux, Asymmetric Hydroformylation. *Chem. Rev.* **95**, 2485-2506 (1995).
13. J. Burés, A. Armstrong, D. G. Blackmond, Kinetic correlation between aldehyde/enamine stereoisomers in reactions between aldehydes with α-stereocenters and chiral pyrrolidine-based catalysts. *Chem. Sci.* **3**, 1273-1277 (2012).
14. L. Zhang, N. Fu, S. Luo, Pushing the limits of aminocatalysis: enantioselective transformations of alpha-branched beta-ketocarbonyls and vinyl ketones by chiral primary amines. *Acc. Chem. Res.* **48**, 986-997 (2015).
15. N. Fu, L. Zhang, J. Li, S. Luo, J. P. Cheng, Chiral primary amine catalyzed enantioselective protonation via an enamine intermediate. *Angew. Chem. Int. Ed.* **50**, 11451-11455 (2011).
16. V. García-López, D. Liu, J. M. Tour, Light-Activated Organic Molecular Motors and Their Applications. *Chem. Rev.* **120**, 79-124 (2020).
17. H. K. Bisoyi, Q. Li, Light-Driven Liquid Crystalline Materials: From Photo-Induced Phase Transitions and Property Modulations to Applications. *Chem. Rev.* **116**, 15089-15166 (2016).
18. D. A. Nicewicz, D. W. MacMillan, Merging photoredox catalysis with organocatalysis: the direct asymmetric alkylation of aldehydes. *Science* **322**, 77-80 (2008).
19. M. T. Pirnot, D. A. Rankic, D. B. Martin, D. W. MacMillan, Photoredox activation for the direct beta-arylation of ketones and aldehydes. *Science* **339**, 1593-1596 (2013).
20. E. Arceo, I. D. Jurberg, A. Alvarez-Fernandez, P. Melchiorre, Photochemical activity of a key donor-acceptor complex can drive stereoselective catalytic alpha-alkylation of aldehydes. *Nat. Chem.* **5**, 750-756 (2013).
21. M. Silvi, E. Arceo, I. D. Jurberg, C. Cassani, P. Melchiorre, Enantioselective organocatalytic alkylation of aldehydes and enals driven by the direct photoexcitation of enamines. *J. Am. Chem. Soc.* **137**, 6120-6123 (2015).
22. J. B. Metternich, R. Gilmour, Photocatalytic *E*→*Z* Isomerization of Alkenes. *Synlett* **27**, 2541-2552 (2016).
23. Y. Li, D. Wang, L. Zhang, S. Luo, Redox Property of Enamines. *J. Org. Chem.* **84**, 12071-12090 (2019).
24. Y. Zhu, L. Zhang, S. Luo, Asymmetric Retro-Claisen Reaction by Chiral Primary Amine Catalysis. *J. Am. Chem. Soc.* **138**, 3978-3981 (2016).
25. K. Singh, S. J. Staig, J. D. Weaver, Facile Synthesis of *Z*-Alkenes via Uphill Catalysis. *J. Am. Chem. Soc.* **136**, 5275-5278 (2014).
26. J. B. Metternich, R. Gilmour, A Bio-Inspired, Catalytic *E*→*Z* Isomerization of Activated Olefins. *J. Am. Chem. Soc.* **137**, 11254-11257 (2015).
27. J. J. Molloy *et al.*, Boron-enabled geometric isomerization of alkenes via selective energy-transfer catalysis. *Science* **369**, 302-306 (2020).

Acknowledgments: We thank Prof. Xingwei Guo and Prof. Lei Jiao for helpful discussions.

Funding: This work is supported by the Natural Science Foundation of China (21672217, 21861132003 and 22031006) and Tsinghua University Initiative Scientific Research Program

for financial support. S.L. is supported by the National Program of Top-notch Young Professionals.

Author contributions: S.L. conceived and directed the project. M.H. conducted the experiments with help of T.P. Z.L. performed the computational studies. M.H. and S.L. wrote the manuscript with contributions from all authors.

Competing interests: Authors declare that they have no competing interests.

Data and materials availability: All data are available in the main text or the supplementary materials.

Supplementary Materials

Materials and Methods

Supplementary Text

Figs. S1 to S18

Tables S1 to S4

References (*S1–15*)